Density functionals for the strong-interaction limit

Michael Seidl,* John P. Perdew, and Stefan Kurth†

Department of Physics and Quantum Theory Group, Tulane University, New Orleans, Louisiana 70118
(Received 20 December 1999; published 7 June 2000)

The strong-interaction limit of density-functional (DF) theory is simple and provides information required for an accurate resummation of DF perturbation theory. Here we derive the point-charge-plus-continuum (PC) model for that limit, and its gradient expansion. The exchange-correlation (xc) energy $E_{xc}[\rho] \equiv \int_0^1 d\alpha W_\alpha[\rho]$ follows from the xc potential energies W_α at different interaction strengths $\alpha \geq 0$ [but at fixed density $\rho(\mathbf{r})$]. For small $\alpha \approx 0$, the integrand W_α is obtained accurately from perturbation theory, but the perturbation expansion requires resummation for moderate and large α. For that purpose, we present density functionals for the coefficients in the asymptotic expansion $W_\alpha \to W_\infty + W'_\infty \alpha^{-1/2}$ for $\alpha \to \infty$ in the PC model. W_∞^{PC} arises from strict correlation, and W'^{PC}_∞ from zero-point vibration of the electrons around their strictly correlated distributions. The PC values for W_∞ and W'_∞ agree with those from a self-correlation-free meta-generalized gradient approximation, both for atoms and for atomization energies of molecules. We also (i) explain the difference between the PC cell and the exchange-correlation hole, (ii) present a density-functional measure of correlation strength, (iii) describe the electron localization and spin polarization energy in a highly stretched H_2 molecule, and (iv) discuss the soft-plasmon instability of the low-density uniform electron gas.

PACS number(s): 31.15.Ew, 31.25.−v, 71.15.Mb

I. INTRODUCTION

In density-functional theory (DFT) [1], the ground-state energy of a system of interacting electrons is presented as a functional of the ground-state density distribution $\rho(\mathbf{r})$ of the electrons,

$$E[\rho] = T_s[\rho] + \int d^3r \rho(\mathbf{r}) v_{ext}(\mathbf{r}) + U[\rho] + E_{xc}[\rho]. \quad (1)$$

$T_s[\rho]$ is the kinetic energy of a system of noninteracting electrons with ground-state density ρ. The second contribution is the interaction with the external potential $v_{ext}(\mathbf{r})$, and $U[\rho] = \frac{1}{2} \int d^3r \int d^3r' \rho(\mathbf{r}) \rho(\mathbf{r}')/|\mathbf{r} - \mathbf{r}'|$ is the classical Hartree-Coulomb energy. The exchange-correlation energy $E_{xc}[\rho]$ accounts for all the complexity of the quantum many-body problem ignored by the continuum functional $U[\rho]$. It also includes the interaction contribution $T_c = \langle \hat{T} \rangle - T_s$ to the kinetic energy.

This important functional is exactly represented by the coupling-constant integral [2,3],

$$E_{xc}[\rho] = \int_0^1 d\alpha W_\alpha[\rho],$$

$$W_\alpha[\rho] = \langle \Psi_\alpha[\rho] | \hat{V}_{ee} | \Psi_\alpha[\rho] \rangle - U[\rho]. \quad (2)$$

The integrand $W_\alpha[\rho]$ (which is plotted approximately in Fig. 1) has only potential-energy contributions, including the expectation value of the Coulomb two-particle repulsion operator $\hat{V}_{ee} = \Sigma_{i<j} |\hat{\mathbf{r}}_i - \hat{\mathbf{r}}_j|^{-1}$ in the ground state $\Psi_\alpha[\rho]$ of a hypothetical system where the repulsion between the electrons

is scaled by a factor ("coupling constant") $\alpha \geq 0$, but which has the same ground-state density $\rho(\mathbf{r})$ as the real system with $\alpha = 1$. In general, $\Psi_\alpha[\rho]$ is that antisymmetrized N-electron wave function which minimizes the expectation value $\langle \hat{T} + \alpha \hat{V}_{ee} \rangle$ and, at the same time, yields the density ρ. If $\Psi_\alpha[\rho]$ is the true ground state of a Hamiltonian with interaction $\alpha \hat{V}_{ee}$,

$$\hat{H}_\alpha = \hat{T} + \alpha \hat{V}_{ee} + \hat{V}_{ext}^\alpha, \quad (3)$$

then the α-dependent external potential $v_{ext}^\alpha(\mathbf{r})$, represented by the operator $\hat{V}_{ext}^\alpha$ in Eq. (3), is completely determined by the density ρ [1]. Note that $W_{\alpha=1}[\rho] = E_{xc}[\rho] - T_c[\rho]$.
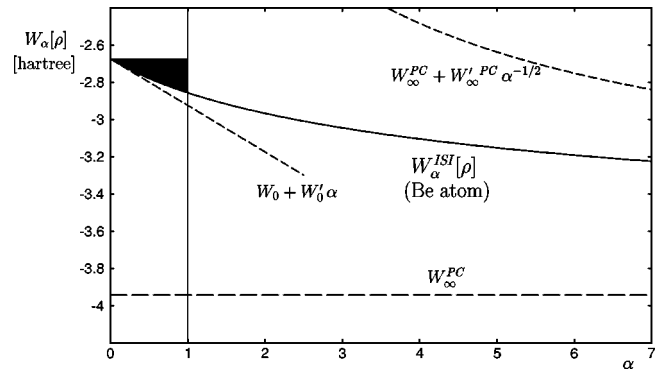

FIG. 1. The ISI model (29) for the coupling-constant integrand of Eq. (2) in the case of the beryllium atom (solid curve; in hartree units). The coefficients W_0, W'_0, W_∞^{PC}, and W'^{PC}_∞ are taken from Table III, using $D = D_2$ for the latter one. The size of the shaded area, which indicates a contribution to the integral (2), is the predicted correlation energy $E_c^{ISI}[\rho] = -0.100$ hartree of the Be atom (exact value: -0.096 hartree). The expansions of W_α^{ISI} both for $\alpha \to 0$ and for $\alpha \to \infty$ are displayed in short dashes. The horizontal dashed line marks the asymptotic limit W_∞^{PC}.

*Present address: Institute of Theoretical Physics, University of Regensburg, D-93040 Regensburg, Germany.

†Present address: Department of Theoretical Physics I, Lund University, Sölvegatan 14 A, S-22362 Lund, Sweden.

The limit $\alpha \to 0$ of weak interaction in the integrand $W_\alpha[\rho]$ of Eq. (2) is well understood. $\Psi_{\alpha=0}[\rho]$ is the Slater determinant of the occupied Kohn-Sham (KS) single-particle orbitals $\{\varphi_i(\mathbf{r},\sigma)\}_{i=1,\ldots,N}$. Correspondingly, $W_{\alpha=0}[\rho]$ is the DFT exchange energy,

$$W_0[\rho] = E_x[\rho] \equiv -\frac{1}{2}\sum_{i,j=1}^{N}\sum_{\sigma}\int d^3r\, d^3r'$$

$$\times \frac{\varphi_i^*(\mathbf{r},\sigma)\,\varphi_j^*(\mathbf{r}',\sigma)\,\varphi_i(\mathbf{r}',\sigma)\,\varphi_j(\mathbf{r},\sigma)}{|\mathbf{r}-\mathbf{r}'|}. \quad (4)$$

The first derivative at $\alpha=0$,

$$W_0'[\rho] \equiv (dW_\alpha[\rho]/d\alpha)_{\alpha=0} = 2E_c^{GL2}[\rho], \quad (5)$$

is, like E_x, also known [4] in terms of the KS orbitals as we shall see in the next paragraph.

In Görling-Levy (GL) perturbation theory [4], the correlation energy $E_c[\rho_\lambda] \equiv E_{xc}[\rho_\lambda] - E_x[\rho_\lambda]$ for the scaled density $\rho_\lambda(\mathbf{r}) \equiv \lambda^3 \rho(\lambda\mathbf{r})$ is expanded around the high-density limit $\lambda \to \infty$ or $\alpha \to 0$ (with $\alpha = 1/\lambda$),

$$E_c[\rho_{1/\alpha}] = \sum_{n=2}^{\infty} E_c^{GL\,n}[\rho]\alpha^{n-2} \quad (\alpha \to 0). \quad (6)$$

A hypothetic system where the electronic repulsion $\hat{V}_{ee}$ is scaled by the factor α has the correlation energy [5]

$$E_c^\alpha[\rho] = \alpha^2 E_c[\rho_{1/\alpha}]. \quad (7)$$

Thus, $E_c^\alpha[\rho] = \sum_{n=2}^{\infty} E_c^{GL\,n}[\rho]\alpha^n$. Since $E_c^\alpha = \int_0^\alpha d\alpha'(W_{\alpha'} - W_0)$, we have $W_\alpha[\rho] = W_0 + \sum_{n=2}^{\infty} E_c^{GL\,n}[\rho]\,n\alpha^{(n-1)}$. Therefore, GL perturbation theory is equivalent to the Taylor expansion of $W_\alpha[\rho]$ around the weak-interaction limit $\alpha = 0$, which implies Eqs. (4) and (5). For an explicit expression of $E_c^{GL2}[\rho]$, see Ref. [4].

It has been shown recently [6,7] that the weak-interaction limit,

$$W_\alpha[\rho] \to W_0[\rho] + W_0'[\rho]\,\alpha \quad (\alpha \to 0), \quad (8)$$

along with some additional information on the opposite limit $\alpha \to \infty$, where $W_\alpha[\rho]$ approaches asymptotically a finite value $W_\infty[\rho]$ (see Fig. 1),

$$W_\alpha[\rho] \to W_\infty[\rho] + W_\infty'[\rho]\,\alpha^{-1/2} \quad (\alpha \to \infty), \quad (9)$$

can be sufficient for an accurate evaluation of the integral (2).

As $\alpha \to \infty$, the external potential $v_{ext}^\alpha(\mathbf{r})$ that holds the density fixed becomes strongly attractive. In fact

$$\lim_{\alpha \to \infty} \frac{v_{ext}^\alpha(\mathbf{r})}{\alpha} = -\int d^3r'\frac{\rho(\mathbf{r}')}{|\mathbf{r}-\mathbf{r}'|} - \frac{\delta}{\delta\rho(\mathbf{r})}W_\infty[\rho], \quad (10)$$

since the Kohn-Sham potential which yields the density $\rho(\mathbf{r})$ for noninteracting electrons is

$$v_{ext}^0(\mathbf{r}) = v_{ext}^\alpha(\mathbf{r}) + \alpha\int d^3r'\frac{\rho(\mathbf{r}')}{|\mathbf{r}-\mathbf{r}'|} + \frac{\delta}{\delta\rho(\mathbf{r})}E_{xc}^\alpha[\rho]; \quad (11)$$

here, $E_{xc}^\alpha[\rho] \equiv \int_0^\alpha d\alpha'\,W_{\alpha'}[\rho] \to \alpha W_\infty$ for $\alpha \to \infty$, which follows from the asymptotic behavior (9).

Unlike the realistic situation at $\alpha = 1$, this strong-interaction limit $\alpha \to \infty$ is also simple, but in a different way than the familiar limit $\alpha \to 0$ of weak interaction. As $\alpha \to \infty$, the electrons become strongly correlated. This situation is modeled by the concept of ''strictly correlated electrons'' (SCE) [6,8,9] which is solved exactly for one-dimensional (1D) systems and, in particular, for any 3D two-electron system with a spherical density distribution $\rho(r)$. In the latter case [6,8], the two electrons always stay on opposite sides of the spherical center. The radial distance r_1 of the first electron strictly dictates that of the second electron, $r_2 = f(r_1)$, by virtue of an exact ''correlation'' function $f(r)$. As a solution of the differential equation $f'(r) = -r^2\rho(r)/f(r)^2\rho(f(r))$, f is unambiguously determined by the density ρ [6,8]. (Apart from the minus sign and the appearance of only one function ρ instead of two, this differential equation coincidentally resembles that of a local scaling transformation [54].) In terms of this function $f(r)$, SCE provides the functional [6,8]

$$W_\infty^{SCE}[\rho] = 2\pi\int_0^\infty dr\frac{r^2\rho(r)}{r+f(r)} - U[\rho], \quad (12)$$

which is probably identical with the unknown exact $W_\infty[\rho]$ for spherical two-electron systems.

In the present paper we give the complete derivation of the point-charge-plus-continuum (PC) model [6,10] which is an approximation to the SCE concept but, in contrast to the latter, is straightforwardly applicable to any three-dimensional (3D) N-electron density $\rho(\mathbf{r})$. The PC model provides the simple explicit density functionals $W_\infty^{PC}[\rho]$ and $W_\infty'^{PC}[\rho]$, see Eqs. (23) and (24) below, for the coefficients in Eq. (9). It generalizes the standard spherical-cell model [11,12] of the Wigner crystal, and has a simple density-gradient expansion. (A constrained search for the strong-interaction limit has been discussed by Valone [13]. Some formal properties of this limit have been discussed by Levy and Perdew [14].)

In Sec. II we derive the functional $W_\infty^{PC}[\rho]$, while in Appendix A we explain the difference between the PC cell and the strong-interaction limit of the exchange-correlation (xc) hole. In Sec. III we consider the situation of large but *finite* $\alpha \gg 1$, and we derive in Appendix C the functional $W_\infty'^{PC}[\rho]$ for the next coefficient in the asymptotic expansion (9). We also discuss approximate self-interaction corrections (SIC's) to the gradient expansion $W_\infty'^{PC}[\rho]$. Using these functionals, we apply in Sec. IV the interaction-strength interpolation (ISI) $W_\alpha^{ISI}[\rho]$ of Ref. [7] between the weak-interaction limit (8) and the strong-interaction limit (9). We obtain accurate correlation energies for those atoms where the coefficient W_0' is known with reliable accuracy. The same method predicts in Ref. [7] remarkably accurate atomization energies for a set

of 18 small molecules; a statistical summary is given in Sec. V, where we also discuss the strong-interaction limit for the atomization energy. We summarize our conclusions in Sec. VI.

The α dependence of $W_\alpha[\rho]$ for specific finite or extended systems has been the subject of several recent investigations within density-functional [15–18] or wave-function [19–22] theories. Exact information about $W_\alpha[\rho]$, e.g., W_0 or W_0 and W_0', has been used to boost the accuracy of density-functional calculations [16–18] along the general direction suggested by Becke [23]. Unlike those approaches, which make use of density functionals for $\alpha \approx 1$, we make use of them for $\alpha \to \infty$.

A density-functional measure of the correlation strength of the physical ($\alpha = 1$) wave function is

$$\frac{W_0 - W_1}{W_0 - W_\infty}. \tag{13}$$

This measure varies between 0 for independent electrons and 1 for strictly correlated ones. For other measures, see Ref. [9].

II. POINT-CHARGE-PLUS-CONTINUUM (PC) MODEL FOR $W_\infty[\rho]$

The integrand $W_\alpha[\rho]$ in Eq. (2) is identical to the total electrostatic potential energy (expectation value) $E_\alpha^{es}[\rho]$ of a fictitious system where discrete point electrons with the antisymmetrized and correlated wave function $\Psi_\alpha[\rho]$ are embedded in a rigid continuous background of positive charge with density $\rho_+(\mathbf{r}) \equiv \rho(\mathbf{r})$, since

$$E_\alpha^{es}[\rho] \equiv \langle \Psi_\alpha[\rho] | \hat{V}_{ee} | \Psi_\alpha[\rho] \rangle - 2U[\rho] + U[\rho] = W_\alpha[\rho]. \tag{14}$$

The three terms of Eq. (14) are, respectively, the electron-electron, electron-background, and background-background interactions. (It does not matter here whether $\Psi_\alpha[\rho]$ — which is defined in Eq. (2) above — is the ground state of this fictitious system or not. The positive background is merely an artifice invoked for the evaluation of $W_\alpha[\rho]$, and should not otherwise be taken seriously. The mock electrostatic energy of Eq. (14) provides a more convincing way to derive the PC model.)

Repeated simultaneous measurements of the N electronic positions in the state $\Psi_\alpha[\rho]$ would yield distribution sets $\{\mathbf{r}_i\}_{i=1,\dots,N}$ of N points which, in the ensemble average, represent the continuous density cloud $\rho(\mathbf{r})$. The classical electrostatic energy of the neutral system composed of the N negative point charges of each set and the continuous positive background yields in the ensemble average the quantity $E_\alpha^{es}[\rho]$. In the limit $\alpha \to \infty$, where the electrons repel each other strongly, the points $\mathbf{r}_i$ in each set of the ensemble are distributed as uniformly as possible over the density $\rho(\mathbf{r})$ without any accidental clustering. (Fluctuations of particle number in any finite volume fragment are strongly suppressed [9] as $\alpha \to \infty$.) In other words, at large α, the continuous positive background is locally neutralized as well as

this can be achieved by discrete negative point charges. Therefore, in a typical distribution set the hypothetical system can be divided up into N neutral cells, one around each electron at $\mathbf{r}_i$ and with zero or weak lower electric multipole moments, so that the interaction between different cells may be neglected. Consequently, the total electrostatic energy of the system, $E_\infty^{es}[\rho]$, is approximately the sum of the energies of these N individual cells.

In the following we present a model for the cell around an electron at position $\mathbf{r}$ in the density ρ. This model cell has the energy $E_{cell}([\rho];\mathbf{r})$. The sum $\Sigma_{i=1}^N E_{cell}([\rho];\mathbf{r}_i)$ for a set $\{\mathbf{r}_i\}$ of electron positions becomes in the ensemble average an integral which is an approximation to the electrostatic energy (14) in the limit $\alpha \to \infty$,

$$W_\infty[\rho] = E_\infty^{es}[\rho] \approx \int d^3r\, \rho(\mathbf{r})\, E_{cell}([\rho];\mathbf{r}). \tag{15}$$

We call this the PC model because Eq. (15) treats one electron as a point charge at position $\mathbf{r}$ and the remaining $N-1$ electrons as a continuous fluid of negative charge which perfectly neutralizes the positive background everywhere except for the region inside the cell around the point electron whose position is averaged over the system. Despite some similarities, the PC cell is *not* a model for the strong-interaction limit of the exchange-correlation hole; see Appendix A. By coincidence, the label PC is sometimes used to mean ''perfect correlation'' [24], the very situation for which our PC model is an approximation.

The key idea is that the electron at $\mathbf{r}$ plus its PC cell should have zero monopole and dipole electrostatic moments. In the local-density approximation (LDA), where the density ρ is assumed to be constant in the vicinity of each electron, the model cell around an electron at $\mathbf{r}$ is a concentric sphere with local radius $r_s(\mathbf{r}) = (3/4\pi)^{1/3}\rho(\mathbf{r})^{-1/3}$. The electrostatic energy of this cell,

$$E_{cell}^{LDA}([\rho];\mathbf{r}) = -\frac{9}{10} r_s(\mathbf{r})^{-1}, \tag{16}$$

is the self-energy $\frac{3}{5} r_s^{-1}$ of the spherical piece of uniform positive background inside the cell plus its interaction $-\frac{3}{2} r_s^{-1}$ with the central point electron.

Beyond the LDA is the gradient expansion approximation (GEA), in which the energy is expanded to second order in the density gradient. We assume the density $\rho(\mathbf{r}+\mathbf{s})$ in the vicinity of an electron at $\mathbf{r}$ to have a constant gradient $\mathbf{\Gamma} \equiv \nabla\rho(\mathbf{r})$,

$$\rho(\mathbf{r}+\mathbf{s}) = \rho_0 + \mathbf{\Gamma} \cdot \mathbf{s}, \tag{17}$$

where $\rho_0 \equiv \rho(\mathbf{r})$ is the density at the position of the point electron. If the gradient $\mathbf{\Gamma}$ is not too strong, $\gamma \equiv \Gamma r_s/\rho_0 \ll 1$ where $r_s = [(4\pi/3)\rho_0]^{-1/3}$, the cell is still approximately spherical. To have zero electric dipole moment, however, a positive spherical cell with a density gradient has its center shifted away from the negative point electron by a small displacement $\mathbf{d}$ (with magnitude d) into the direction of $-\mathbf{\Gamma}$ (see Fig. 2). Still normalized to unity, the cell has now a
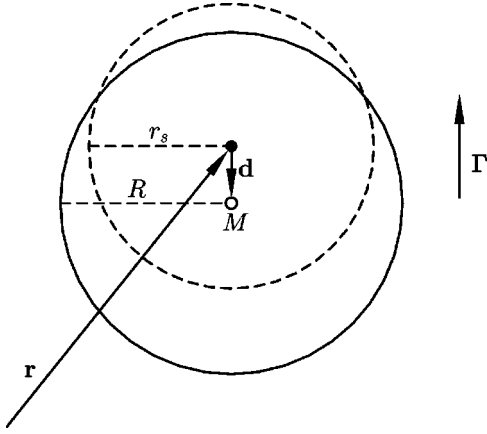
FIG. 2. In a constant density ($\Gamma=0$), the PC cell around an electron at **r** is a concentric sphere with radius r_s, represented by the dashed large circle in the figure. In the presence of a density gradient Γ, however, the center M of the cell is shifted away from the electron by a small displacement vector **d** in the direction of $-\Gamma$. To have zero monopole and dipole moments, the shifted cell (solid large circle in the figure) has a different radius $R>r_s$.

radius $R>r_s$, fixed by $(4\pi/3)R^3\rho_c=1$, where $\rho_c=\rho_0-\Gamma d$ $\equiv\rho_0(1-\gamma d/r_s)$ is the density at the center of the cell.

In a coordinate system which has its origin $\mathbf{u}=0$ at the center of the cell and its u_3 axis in the direction of Γ, the electron is at $\mathbf{u}=-\mathbf{d}=(0,0,+d)$; see Fig. 2. The condition of zero dipole moment is $\int_{-R}^{R}du_3[\pi(R^2-u_3^2)(\rho_c+\Gamma u_3)-\delta(u_3-d)]u_3=0$. This and the normalization condition $(4\pi/3)R^3\rho_c=1$ can be written as

$$R^2=5r_s\frac{d}{\gamma}\left(1-\gamma\frac{d}{r_s}\right)\quad\text{and}\quad R^2=r_s^2\left(1-\gamma\frac{d}{r_s}\right)^{-2/3},$$

(18)

respectively. Expanding $d=d_1\gamma+d_2\gamma^2+\cdots$ in each of these equations and comparing coefficients, we find

$$d(\mathbf{r})=r_s(\tfrac{1}{5}\gamma+\tfrac{1}{15}\gamma^3)+O(\gamma^5),$$

$$R(\mathbf{r})=r_s(1+\tfrac{1}{15}\gamma^2)+O(\gamma^4),$$

(19)

where $r_s=(3/4\pi)^{1/3}\rho(\mathbf{r})^{-1/3}$ and $\gamma=r_s(\mathbf{r})|\nabla\rho(\mathbf{r})|/\rho(\mathbf{r})$ depend on the position $\mathbf{r}$ of the point electron. The two quantities (19) determine both position and size of the spherical PC cell, depending on the position $\mathbf{r}$ of the point electron.

Again, as in the LDA (16), the energy of the PC cell with constant gradient is the self-energy U_{cell} of the piece of positive background inside the cell plus its interaction with the point electron,

$$E_{cell}^{GEA}([\rho];\mathbf{r})=U_{cell}-\Phi_{cell}^{(\mathbf{r})}(\mathbf{u}=-\mathbf{d}(\mathbf{r})).$$

(20)

$\Phi_{cell}^{(\mathbf{r})}(\mathbf{u})$ is the electrostatic potential at $\mathbf{u}$ of the positive background, with $\mathbf{u}=0$ at the center of the cell. Using for U_{cell} and $\Phi_{cell}^{(\mathbf{r})}(\mathbf{u})$ the expressions (B6) and (B4) from Appendix B, with $(4\pi/3)R^3\rho_c=1$, we obtain

$$E_{cell}^{GEA}([\rho];\mathbf{r})=\left[\frac{3}{5}+\frac{1}{35}\left(\frac{\Gamma R}{\rho_c}\right)^2\right]R^{-1}$$

$$-\left[\frac{1}{2}\left(3-\frac{d^2}{R^2}\right)+\frac{1}{10}\frac{\Gamma d}{\rho_c}\left(5-3\frac{d^2}{R^2}\right)\right]R^{-1}.$$

(21)

Using $\Gamma d/\rho_c=\frac{1}{5}\gamma^2+O(\gamma^4)$ and the expansions (19), we find, in generalization of Eq. (16),

$$E_{cell}^{GEA}([\rho];\mathbf{r})=\left(-\frac{9}{10}+\frac{3}{350}\gamma^2\right)r_s(\mathbf{r})^{-1}+O(\gamma^4).$$

(22)

Applying the model (15) and neglecting contributions of order γ^4, we obtain the PC GEA

$$W_\infty^{PC}[\rho]=\int d^3r\left\{A\,\rho(\mathbf{r})^{4/3}+B\,\frac{|\nabla\rho(\mathbf{r})|^2}{\rho(\mathbf{r})^{4/3}}\right\},$$

(23)

for the unknown functional $W_\infty[\rho]$. The coefficients are $A=-(9/10)(4\pi/3)^{1/3}=-1.451$ and $B=(3/350)(3/4\pi)^{1/3}=5.317\times10^{-3}$. The functional (23) has the correct scaling behavior, $W_\infty^{PC}[\rho_\lambda]=\lambda W_\infty^{PC}[\rho]$, as predicted in Eq. (31).

The standard local-density approximation for E_{xc} is not accurate in the limit $\alpha\to\infty$, because of a serious self-correlation error which develops in that limit. As a result, this approximation [as well as the generalized gradient approximation (GGA)] cannot properly describe the Wigner crystallization of the low-density uniform electron gas [25]. The strongly interacting limit of the PBE GGA is essentially local and spin independent, as shown by the flatness of the $r_s=\infty$ enhancement factors in Fig. 1 of Ref. [26]: $W_\infty^{GGA}[\rho_\uparrow,\rho_\downarrow]\approx W_\infty^{LSD}[\rho_\uparrow,\rho_\downarrow]\approx 2E_x^{LDA}[\rho]$. (Although LDA and GGA *exchange* energies suffer a self-interaction error, this error is typically small and does not change as $\Psi_\alpha[\rho]$ approaches the strong-interaction limit. The LDA and GGA *correlation* energies suffer a self-interaction error which grows alarmingly towards this limit.)

However, we can test the accuracy of the functional (23) against the meta-generalized gradient approximation (MGGA) for the correlation energy [27], which is constructed from first principles without adjusting any parameters to experimentally known data. MGGA yields accurate energies for very different kinds of electronic systems such as atoms, molecules, solids, and surfaces. Due to its exact self-correlation correction (SIC), MGGA should work particularly well in the strong-interaction limit, where LDA and GGA do not. MGGA has an extra ingredient: not only the local density and its gradient, but also the orbital kinetic energy density.

For a set of 12 atoms, Table I gives a comparison of $W_\infty^{PC}[\rho]$ with the functional $W_\infty^{MGGA}[\rho]$ which is the model for $W_\infty[\rho]$ as extracted (Appendix D) from the MGGA functional. The good agreement of the results from the PC model with the ones from the MGGA functional in Table I is particularly encouraging, since two completely independent approaches to the strong-interaction limit are compared here.

TABLE I. Values for $W_\infty[\rho]$ (in units of 1 hartree = 27.21 eV) for atoms, obtained for exchange-only Krieger, Li, and Iafrate (KLI) [50] densities from the LSD, GGA, and MGGA functionals (Appendix D) and from the PC model.

Atom	W_∞^{LSD}	W_∞^{GGA}	W_∞^{MGGA}	W_∞^{PC}
H	-0.421	-0.417	-0.308	-0.313
He	-1.720	-1.689	-1.502	-1.463
Li	-2.958	-2.904	-2.575	-2.557
Be	-4.504	-4.424	-3.955	-3.947
N	-11.176	-11.048	-10.043	-10.187
Ne	-21.469	-21.294	-19.752	-20.018
Na	-24.848	-24.652	-22.916	-23.261
Mg	-28.435	-28.224	-26.298	-26.702
P	-40.298	-40.055	-37.524	-38.101
Ar	-54.240	-53.946	-50.831	-51.562
Kr	-172.467	-172.002	-165.355	-167.334
Xe	-331.981	-331.355	-321.204	-324.524

The true functional $W_\infty[\rho]$ is known exactly in two particular cases: For one-electron systems (like the H atom in Table I), $W_\alpha[\rho] \equiv -U[\rho]$, for all $\alpha \geq 0$. For the H atom, $\rho(\mathbf{r}) = e^{-2r}/\pi$ and $-U[\rho] = -\frac{5}{16} = -0.3125$ which is reproduced almost perfectly by the PC model and, as a result of the self-correlation correction, accurately by the MGGA approach. For spherical two-electron systems (like the He atom in Table I), the strong-interaction limit is probably exactly solved by the concept of strictly correlated electrons (SCE) [6,8] which by Eq. (12) predicts $W_\infty[\rho_{He}] = -1.500$ for the He density used in Table I.

In density-functional theory, gradient expansions like Eq. (23) are usually constructed to be exact to order $|\nabla\rho|^2$ for slowly varying densities, and often fail (unless suitably generalized [28]) for realistic densities. However, because our Eq. (23) is derived differently, it need not share any of these features with traditional gradient expansions. In particular, the PC cell to order $|\nabla\rho|^2$ is properly normalized, Eq. (A2) of Appendix A, while the exchange-correlation hole to order $|\nabla\rho|^2$ is not [28]. Thus, we do not necessarily interpret the coefficient B of Eq. (23) as the low-density limit of the second-order gradient coefficient of $E_{xc}[\rho]$ for a slowly varying density ρ. The high-density limit of this coefficient is believed to be $1.854 \times 10^{-3} = -2.381 \times 10^{-3} + 4.235 \times 10^{-3}$, where the first term is from exchange [29] and the second from correlation [30–32]. In Appendix E we use Eq. (23) to investigate the soft-plasmon instability of the low-density uniform electron gas against the formation of static charge-density waves.

III. MODELS FOR THE COEFFICIENT $W_\infty'[\rho]$

Strongly interacting electrons at large but *finite* $\alpha \gg 1$ are expected to exhibit a zero-point vibration around their strictly correlated distribution at $\alpha = \infty$ [8]. While strictly correlated electrons at $\alpha = \infty$ are moving on a constant potential-energy surface, the zero-point vibration at finite $\alpha \gg 1$ is driven by a strong oscillator-type effective potential of

the order α [8]. We therefore expect that the strongly correlated motion of the electrons at large $\alpha \gg 1$ can be understood in terms of a slow strictly correlated motion, superimposed by fast small-amplitude collective oscillations. Correspondingly, as in the Born-Oppenheimer treatment of the nuclear motion in molecules, we take the strictly correlated motion as infinitely slow and consider oscillations in an otherwise static array of electrons.

If all the electrons are strictly correlated, then the net force on one electron at $\mathbf{r}$ [due to the other $N-1$ electrons and the external potential $v_{ext}^\alpha(\mathbf{r})$] vanishes to order α, and this remains true when the electron moves to $\mathbf{r}+\mathbf{s}$. But suppose that the other $N-1$ electrons do not follow. Then there is a restoring force which drives the electron back to $\mathbf{r}$.

We demonstrate in Appendix C how the PC approximation (15) for the limit $\alpha \to \infty$ can be generalized to the present situation with oscillations at large but finite $\alpha \gg 1$. $W_\alpha[\rho]$ can still be evaluated exactly as the electrostatic energy (14) with a positive background. The restoring force mentioned in the preceding paragraph, however, is not affected by this positive background which is entirely fictitious. This force is due only to the repulsion by the other $N-1$ electrons plus the unknown external potential $v_{ext}^\alpha(\mathbf{r})$. In Appendix C we present the PC model for $-\nabla v_{ext}^\alpha(\mathbf{r})$ and the restoring force on the electron. Then, with the modified charge distribution of an oscillating electron, Eq. (15) yields $W_\alpha[\rho] \approx W_\infty^{PC}[\rho] + W_\infty'^{PC}[\rho]\,\alpha^{-1/2}$ ($\alpha \gg 1$), where the coefficient $W_\infty'^{PC}[\rho]$, like $W_\infty^{PC}[\rho]$ in Eq. (23), is obtained as a gradient expansion,

$$W_\infty'^{PC}[\rho] = \int d^3r \left\{ C\,\rho(\mathbf{r})^{3/2} + D\,\frac{|\nabla\rho(\mathbf{r})|^2}{\rho(\mathbf{r})^{7/6}} \right\}. \quad (24)$$

This is the *PC* GEA for the coefficient $W_\infty'[\rho]$ in Eq. (9).

The LDA coefficient in Eq. (24) is $C = \frac{1}{2}(3\pi)^{1/2} = 1.535$, in agreement with the spherical-cell treatment of the zero-point vibration in a Wigner-crystal in Ref. [12]. To provide an approximate self-interaction correction (SIC) for one-electron densities for which the true functional $W_\infty'[\rho]$ is exactly zero, the gradient correction in Eq. (24) should have a sign opposite to that of the LDA term. Our derivation in Appendix C, however, yields the small but positive number $D_0 = \frac{1}{40}(3/4\pi)^{1/6} = 0.0197$ for the coefficient D. Unless there is a mistake in Appendix C, the effective PC gradient coefficient D for small density gradients is positive, while that for typical gradients is negative (as estimated in the next paragraph).

Formally, however, the functional (24) has the correct [8] scaling behavior of the true functional $W_\infty'[\rho]$, $W_\infty'^{PC}[\rho_\lambda] = \lambda^{3/2} W_\infty'^{PC}[\rho]$. Therefore, we can keep Eq. (24) and determine a more realistic value for the coefficient D from a physically motivated condition. If we put, e.g., $D = D_1 = -0.030\,676$, expression (24) is identically zero for any *exponential* (i.e., hydrogenic) one-electron spherical density $\rho(r) = \lambda^3 e^{-2\lambda r}/\pi$ ($\lambda > 0$). In Table II we compare the values $W_\infty'^{PC}[\rho]$ with the corresponding values of the functional $W_\infty'^{MGGA}[\rho]$ which is extracted (Appendix D) from the MGGA exchange-correlation functional of Ref. [27]. In all

TABLE II. Values for $W'_\infty[\rho]$ (in units of 1 hartree = 27.21 eV) for atoms, obtained from the LSD, GGA, and MGGA functionals (Appendix D) and from the PC model. The local term in the LSD, GGA, and MGGA has been slightly modified here to agree with the local term in the PC model. See the caption of Table I.

Atom	W'^{LSD}_∞	W'^{GGA}_∞	W'^{MGGA}_∞	W'^{PC}_∞
H	0.257	0.243	0.000	0.043
He	1.553	1.516	0.728	0.729
Li	3.252	3.176	1.532	1.623
Be	5.561	5.448	2.723	2.919
N	16.512	16.344	9.642	10.176
Ne	35.483	35.283	23.886	24.425
Na	42.966	42.745	29.586	30.115
Mg	51.115	50.886	35.867	36.352
P	79.473	79.202	58.244	58.378
Ar	114.391	114.082	86.761	86.179
Kr	463.955	463.481	390.997	381.015
Xe	1042.900	1042.223	914.250	886.290

tables, we have put $D=D_2=-0.025\,58$, which is chosen so that $W'^{PC}_\infty[\rho]$ and $W'^{MGGA}_\infty[\rho]$ agree for the two-electron density of the He atom.

Functionals of the form (23) and (24) are at least potentially exact for the electron gas of uniform density. While we have no exact solution for the strong-interaction or low-density limit, the SCE energy should be close to that of a bcc Wigner crystal [33–35],

$$E^W_{xc} = -\frac{0.89593}{r_s} + \frac{1.325}{r_s^{3/2}} + \cdots. \quad (25)$$

This is not far from the prediction of Eqs. (2), (9), (23), and (24) for the uniform gas as $r_s \to \infty$,

$$E_{xc} = -\frac{0.900\,00}{r_s} + \frac{1.500}{r_s^{3/2}} + \cdots. \quad (26)$$

The closeness of the energies for the Wigner crystal and for the uniform gas as $r_s \to \infty$ has been observed elsewhere [36,37].

The accuracy of gradient-corrected functionals can sometimes be improved by using the separate up- and down-spin densities instead of the total density, but this is not the case for our Eqs. (24) and (23), which assume that two electrons cannot be found together at the same point in space. The functionals $W_\infty[\rho]$ and $W'_\infty[\rho]$ are in fact the same for bosons as for fermions.

IV. CORRELATION ENERGIES OF ATOMS

We can use the results from Tables I and II to evaluate the "interaction strength interpolation" (ISI) functional for the correlation energy of Ref. [7], $E^{ISI}_c[\rho] = E^{ISI}_{xc}[\rho] - E_x[\rho]$, using information only on the relatively simple extreme limits $\alpha \to 0$ and $\alpha \to \infty$,

$$E^{ISI}_{xc}[\rho] = W_\infty + \frac{2X}{Y}\left[(1+Y)^{1/2} - 1 - Z\ln\left(\frac{(1+Y)^{1/2}+Z}{1+Z}\right)\right], \quad (27)$$

where the coefficients require information only on the weak- and strong-interaction limits,

$$X[\rho] = \frac{xy^2}{z^2}, \quad Y[\rho] = \frac{x^2y^2}{z^4}, \quad Z[\rho] = \frac{xy^2}{z^3} - 1, \quad (28)$$

with $x = -2W'_0[\rho]$, $y = W'_\infty[\rho]$, and $z = W_0[\rho] - W_\infty[\rho]$. Table III summarizes the results for some cases in which the coefficient $W'_0[\rho]$ is known with reliable accuracy [51]. (For the atoms not shown in Table III, the core-core contribution to $W'_0[\rho]$ is not accurately known.)

Equation (27) is obtained in Ref. [7] by analytical integration, according to Eq. (2), of the ISI model for the integrand $W_\alpha[\rho]$,

$$W^{ISI}_\alpha[\rho] = W_\infty[\rho] + \frac{X[\rho]}{\sqrt{1+Y[\rho]\,\alpha} + Z[\rho]}. \quad (29)$$

TABLE III. Increasingly accurate approximations to the correlation energy (in units of 1 hartree = 27.21 eV) of atoms with KLI [50] densities and the two-electron system with exponential density $\rho(r) = 2\exp(-2r)/\pi$ (labeled as Exp.), using information only on the extreme limits $\alpha \to 0$ and $\alpha \to \infty$. $E^{GL2}_c[\rho] \equiv \frac{1}{2}W'_0[\rho]$ is the second-order correlation energy (calculated with GGA densities) in Görling-Levy perturbation theory ([51] and, for Exp., Ref. [21]; for He, the value $W'_0[\rho] = -0.048$ is obtained if a KLI density is used [52]). $E^{ISI,0}_c[\rho]$ is the correlation energy of Ref. [6], which includes information on the strong-interaction limit $\alpha \to \infty$, provided by the PC model $W^{PC}_\infty[\rho]$. In further improvement of these results toward the exact $E^{exact}_c[\rho]$, we also list the values $E^{ISI}_c[\rho]$, obtained with the present exchange-correlation functional, Eq. (27), which in addition includes the information provided by the asymptotic coefficient $W'^{PC}_\infty[\rho]$. $\tilde{W}'_\infty[\rho] = [(W_0 - W_\infty)^3/(-2W'_0)]^{1/2}$ is the estimate of Ref. [6] for $W'_\infty[\rho]$.

System	W_0	W'_0	$E^{GL2}_c \equiv \frac{1}{2}W'_0$	W^{PC}_∞	$E^{ISI,0}_c$	$\tilde{W}'_\infty$ [6]	W'^{PC}_∞	E^{ISI}_c	E^{exact}_c
He	−1.025	−0.101	−0.050	−1.463	−0.041	0.647	0.729	−0.041	−0.042
Exp.	−0.625	−0.093	−0.047	−0.886	−0.035	0.309	0.345	−0.034	−0.037
Be	−2.674	−0.250	−0.125	−3.943	−0.105	2.022	2.919	−0.100	−0.096
Ne	−12.084	−0.938	−0.469	−20.018	−0.420	16.323	24.425	−0.405	−0.394

This analytic function is plotted in Fig. 1. The choice (28) of the coefficients guarantees that the model (29) has the exact asymptotic properties (8) and (9).

Note that $x, y, z \geq 0$, and that $dW_\alpha^{ISI}/d\alpha < 0$ and $d^2 W_\alpha^{ISI}/d\alpha^2 > 0$ for $\alpha \geq 0$. Note also that $W_\alpha^{ISI}[\rho]$ remains finite even when $W_0' \to -\infty$,

$$\lim_{W_0' \to -\infty} W_\alpha^{ISI} = W_\infty + \frac{W_0 - W_\infty}{1 + \dfrac{W_0 - W_\infty}{W_\infty'}\sqrt{\alpha}}; \qquad (30)$$

the interpolation (29) does not break down completely even for metals, although it is more appropriate to finite systems or to insulators where W_0' is finite. Equations (29) and (28) generalize Eqs. (7) and (8) of Ref. [6], in which $Z[\rho] = 0$ so that $W_\infty'[\rho]$ cannot be chosen independently but is fixed by $W_\infty'[\rho] = \{(W_0 - W_\infty)^3/(-2W_0')\}^{1/2}$; see Fig. 4 of Ref. [8].

Our functionals (23) and (24) have the scaling behavior

$$W_\infty^{PC}[\rho_\lambda] = \lambda W_\infty^{PC}[\rho], \quad W_\infty'^{PC}[\rho_\lambda] = \lambda^{3/2} W_\infty'^{PC}[\rho], \qquad (31)$$

where the scaled density $\rho_\lambda(\mathbf{r}) \equiv \lambda^3 \rho(\lambda \mathbf{r})$ is generated from a given density $\rho(\mathbf{r})$ by a scaling factor $\lambda > 0$. Since $W_0[\rho_\lambda] = \lambda W_0[\rho]$ and $W_0'[\rho_\lambda] = W_0'[\rho]$, the relations (31) guarantee that our model integrand (29) fulfills

$$W_\alpha^{ISI}[\rho] = \alpha W_{\alpha=1}^{ISI}[\rho_{\lambda=1/\alpha}], \qquad (32)$$

which is a key property [5] of the unknown exact integrand $W_\alpha[\rho]$. Equation (32) shows in particular how the strong-interaction limit ($\alpha \to \infty$) is related to the low-density limit ($\lambda \to 0$). A graphical illustration of the integrand $W_\alpha^{ISI}[\rho]$ with its integral is displayed in Fig. 1, for which the four functionals $W_0[\rho]$, $W_0'[\rho]$, $W_\infty'^{PC}[\rho]$, and $W_\infty^{PC}[\rho]$ have been evaluated with an accurate ground-state density ρ_{Be} of the beryllium atom.

An important property of the exact $E_{xc}[\rho]$ is its size consistency: $E_{xc}[\rho_1 + \rho_2] = E_{xc}[\rho_1] + E_{xc}[\rho_2]$ for two well-separated densities ρ_1 and ρ_2. Because our inputs $W_0[\rho]$, $W_0'[\rho]$, $W_\infty[\rho]$, and $W_\infty'[\rho]$ are size consistent, so is our $W_\alpha^{ISI}[\rho]$ in the weak- and strong-interaction limits. But, because Eqs. (29) and (27) are nonlinear, our $E_{xc}^{ISI}[\rho]$ is not generally size consistent (although it behaves properly for $\rho_1 = \rho_2$). This failure could be mild, since it arises from the uncertainty in our interpolation formula of Eq. (29). To achieve full size consistency, we could make our interpolation not globally but at each point $\mathbf{r}$ of space.

V. ATOMIZATION ENERGIES IN THE INTERACTION STRENGTH INTERPOLATION AND IN THE STRONG-INTERACTION LIMIT

We have calculated atomization energies for 18 small molecules within the ISI model of Eq. (27) in Ref. [7]. The model accurately reproduces the experimental atomization energies with a mean absolute error of only about 4 kcal/mole = 0.006 hartree or 2.8% of the mean experimental at-

TABLE IV. Signed mean errors (sme) and mean absolute errors (mae) in kcal/mole of the atomization energies of the 18 small molecules studied in Ref. [7] (and listed explicitly in Tables V and VI) in LSD, GGA, meta-GGA, unrestricted Hartree-Fock (HF), second-order Görling-Levy perturbation theory (GL2), and the ISI model. For the traditional density-functional methods (LSD, GGA, meta-GGA), the energies were taken from the work of Refs. [26,27] and [42]. For the exact-exchange methods (HF, GL2, ISI), the HF and GL2 input was taken from Ref. [17], and the ISI energies from Ref. [7]. (1 kcal/mole = 0.0434 eV = 1.594 millihartree.)

	LSD	GGA	MGGA	HF	GL2	ISI
sme	31.2	8.3	1.6	-65.7	74.3	1.9
mae	31.2	9.7	4.1	66.1	74.3	4.3

omization energy. This accuracy is even more remarkable for the fact that it was achieved without the typical cancellation of errors between the exchange and the correlation energies exhibited by density functionals like LSD or GGA, because the ISI model makes use of the exact exchange energy. In Ref. [42] we found a similar interpolation error for the ISI model when all the input quantities were calculated within the meta-GGA.

For the 18 molecules studied in Ref. [7], Table IV compares the (signed) mean and mean absolute errors of the atomization energies in LSD, GGA, meta-GGA, HF (unrestricted Hartree-Fock), second-order Görling-Levy (GL2), and ISI. While HF underbinds severely and GL2 overbinds severely, ISI is rather realistic.

For this work we have studied the change upon atomization of W_∞ and W_∞' within the different density-functional approximations. The results are shown in Tables V and VI, respectively. Similar to the results for atoms, the meta-GGA typically gives a much closer agreement for ΔW_∞ with the PC model than both LSD and GGA (which yield results very similar to one another). This is probably due to the fact that the meta-GGA is self-correlation-free while LSD and GGA are not. It should be kept in mind, however, that the meta-GGA exchange is not exactly self-interaction free.

For the change upon atomization of W_∞', we find that for most cases meta-GGA gives the best agreement with the PC model. Although the agreement is not quite as good as for the changes of W_∞ upon atomization, it is still satisfactory considering the fact that the meta-GGA was not constructed with the strong-interaction limit in mind. Again, LSD and GGA give results which are rather close to one another.

As is evident from Fig. 1, the total exchange-correlation energy E_{xc} of an atom is close to its weak-interaction limit E_x and far from its strong-interaction limit W_∞. But the atomization energy of a molecule is close to *neither* limit. For the 18 molecules in Tables V and VI, the weak-interaction limit (exact E_x and no correlation) underbinds by an average 66 kcal/mole = 0.11 hartree or 44%, while the strong-interaction limit (W_∞^{PC}) overbinds by an average 336 kcal/mole = 0.54 hartree or 222% of the mean experimental atomization energy.

For most electronic systems, strong interaction is of interest only as a limit. The heavier and more classical ions in a low-temperature plasma or liquid metal come much closer to

TABLE V. Changes upon atomization, ΔW_∞ $= W_\infty$(separated atoms)$- W_\infty$(molecule) (in units of 1 hartree $=27.21$ eV), of the exchange-correlation functional in the strongly interacting limit in LSD, GGA, and meta-GGA (Appendix D) and within the PC model. The functionals were evaluated with self-consistent GGA densities at experimental geometries. The calculations were performed using a modified version of the CADPAC program [53].

Molecule	ΔW_∞^{LSD}	ΔW_∞^{GGA}	ΔW_∞^{MGGA}	ΔW_∞^{PC}
H_2	0.273	0.260	0.352	0.313
LiH	0.224	0.219	0.264	0.258
Li_2	0.078	0.078	0.097	0.111
LiF	0.533	0.536	0.570	0.616
Be_2	0.078	0.083	0.095	0.122
CH_4	1.252	1.247	1.556	1.536
NH_3	1.065	1.062	1.329	1.293
OH	0.391	0.389	0.521	0.473
H_2O	0.801	0.795	1.042	0.973
HF	0.454	0.450	0.570	0.551
B_2	0.266	0.277	0.360	0.375
CN	0.664	0.679	0.773	0.806
CO	0.743	0.748	0.895	0.891
N_2	0.808	0.818	0.918	0.942
NO	0.659	0.666	0.798	0.801
O_2	0.536	0.540	0.722	0.689
O_3	0.857	0.860	1.163	1.142
F_2	0.272	0.269	0.340	0.384

TABLE VI. Changes upon atomization, $\Delta W_\infty'$ $= W_\infty'$(separated atoms)$- W_\infty'$(molecule) (in units of 1 hartree $=27.21$ eV), in LSD, GGA, and meta-GGA (Appendix D) and within the PC model. See the caption of Table V.

Molecule	$-\Delta W_\infty'^{LSD}$	$-\Delta W_\infty'^{GGA}$	$-\Delta W_\infty'^{MGGA}$	$-\Delta W_\infty'^{PC}$
H_2	0.276	0.281	0.367	0.270
LiH	0.183	0.193	0.237	0.197
Li_2	0.055	0.062	0.077	0.086
LiF	0.497	0.528	0.723	0.692
Be_2	0.044	0.053	0.116	0.120
CH_4	1.223	1.282	1.950	1.683
NH_3	1.083	1.130	1.739	1.485
OH	0.413	0.430	0.771	0.570
H_2O	0.849	0.884	1.539	1.182
HF	0.502	0.523	0.874	0.705
B_2	0.228	0.257	0.515	0.465
CN	0.691	0.735	1.058	1.089
CO	0.828	0.870	1.369	1.238
N_2	0.908	0.949	1.254	1.290
NO	0.731	0.767	1.209	1.127
O_2	0.585	0.620	1.240	1.003
O_3	0.918	0.976	1.980	1.639
F_2	0.293	0.316	0.599	0.551

this limit. However, the spin-polarization energy of the hydrogen atom provides an example of strong electronic correlation. For a fully spin-polarized hydrogen atom, the exact W_α is -0.3125 hartree for all $\alpha \geq 0$, an uncorrelated situation that can be described accurately by our ISI of Eq. (29). An unpolarized hydrogen atom can be regarded as half of a ground-state H_2 molecule with a highly stretched bond length; its exact W_α is $-0.156\,25$ hartree for $\alpha=0$, but -0.3125 hartree for any $\alpha>0$, since any positive α will switch the stretched-H_2 wave function Ψ_α from Hartree-Fock to Heitler-London form (the latter with localized electrons and zero probability for finding both electrons on the same atom), and this strong-correlation situation is *not* accurately approximated by our ISI of Eq. (29). (Note that it is the ISI and not the PC model that fails here.) While the true spin-polarization energy is zero, the ISI places the unpolarized atom 1.3 eV higher in energy than the polarized one. This is a remarkably persistent error: 1.0 eV in LSD, 1.2 eV in GGA, and 1.0 eV in meta-GGA. For an explanation how spurious spin polarization can mimic strong correlation, see Ref. [38].

VI. CONCLUSIONS

Standard density functionals for the exchange-correlation energy (the local density approximation and the generalized gradient approximation) fail in the strong-interaction or low-density limit as a result of self-interaction error [25]. Thus, to

describe real strongly correlated systems like transition-metal oxides, one needs a self-interaction correction [39] or Hubbard U [40].

However, we have found good agreement in this limit between the meta-generalized gradient expansion of Ref. [27], which is exactly self-correlation free, and our PC gradient expansions of Eqs. (23) and (24), which are approximately self-correlation-free. Thus, we suspect that the low-density limit is under control, and that it should be possible to use the meta-GGA to study, for example, the Wigner crystallization of the uniform electron gas.

The agreement between the PC gradient expansion and the meta-GGA in the strong-interaction limit is remarkable, as these are very different approximations derived in different ways and from different ingredients. The agreement found here for atoms and molecules cannot persist for very rapidly varying densities, such as those of narrow quantum wells [41], where large reduced density gradients can make W_∞^{PC} improperly positive and $W_\infty'^{PC}$ improperly negative.

Our Eqs. (23) and (24) can be used along with GL2 perturbation theory in the ''interaction strength interpolation'' of Eqs. (27) and (29). Accurate correlation energies are found both for atoms (this work) and molecules (Ref. [7]). As explained in Ref. [7], the ISI correlation energy functional is compatible with exact exchange, in a way that standard density functionals are not. The ISI of Eq. (27) also provides an estimate [7] for the radius of convergence of density-functional perturbation theory. The ISI interpolation error has been estimated [42] to be 0.1% for the exchange-correlation energy of an atom and 4 kcal/mole$=0.17$ eV for the atomization energy of a molecule, via tests made within the meta-generalized gradient approximation. For the uni-

form electron gas, ISI predicts a correlation energy which is finite but (except at low densities) inaccurate [42]. For a uniform gas with an artificially imposed energy gap [43], it becomes increasingly accurate as the gap increases.

We have further explained the point-charge-plus-continuum (PC) model which is the basis for Eqs. (23) and (24). The mock electrostatic energy of Eq. (14) is evaluated in the strongly interacting limit by dividing the system up into nonoverlapping, neutral, weakly interacting cells. Despite some similarities, the PC cell is *not* the strongly interacting limit of the exchange-correlation hole (Appendix A), because the exchange-correlation holes overlap even in this limit. The relatively short range of the PC cell helps to explain the accuracy of a second-order gradient expansion in the strongly interacting limit.

APPENDIX A: EXCHANGE-CORRELATION HOLE VERSUS PC CELL

The density $n_{xc}(\mathbf{r},\mathbf{r}')$ at $\mathbf{r}'$ of the *exchange-correlation hole* [3] around an electron at $\mathbf{r}$ is defined such that $\tilde{\rho}(\mathbf{r}') \equiv [\rho(\mathbf{r}') + n_{xc}(\mathbf{r},\mathbf{r}')]$ is the effective charge density, seen by the electron due to the $N-1$ other electrons. ''Effective charge density'' means that the two contributions to the energy functional (1) that describe the electron-electron interaction can be written in the Hartree form

$$U[\rho] + E_{xc}[\rho] = \tfrac{1}{2} \int d^3r\, \rho(\mathbf{r}) \int d^3r' \frac{[\rho(\mathbf{r}') + n_{xc}(\mathbf{r},\mathbf{r}')]}{|\mathbf{r}-\mathbf{r}'|}. \tag{A1}$$

Note, however, that $\tilde{\rho}(\mathbf{r}')$ also accounts for the kinetic-energy contribution $T_c[\rho] = \langle \hat{T} \rangle - T_s[\rho]$ in $E_{xc}[\rho]$.

Here we discuss the relationship between the exchange-correlation hole $n_{xc}(\mathbf{r},\mathbf{r}')$ and the density shift $n_{PC}(\mathbf{r},\mathbf{r}')$ that arises at $\mathbf{r}'$ due to the creation of a PC cell around an electron at $\mathbf{r}$. Both are normalized to -1,

$$\int d^3r'\, n_{xc}(\mathbf{r},\mathbf{r}') = \int d^3r'\, n_{PC}(\mathbf{r},\mathbf{r}') = -1, \tag{A2}$$

and for strong interaction both tend to $-\rho(\mathbf{r})$ as $\mathbf{r}' \to \mathbf{r}$. Both give E_{xc} in the strongly interacting limit (where $E_{xc}[\rho] = W_{\infty}[\rho]$), but *not* in the same way,

$$E_{xc} = \tfrac{1}{2} \int d^3r\, \rho(\mathbf{r}) \int d^3r' \frac{n_{xc}(\mathbf{r},\mathbf{r}')}{|\mathbf{r}-\mathbf{r}'|}$$

$$= \int d^3r\, \rho(\mathbf{r}) \int d^3r' \frac{n_{PC}(\mathbf{r},\mathbf{r}')}{|\mathbf{r}-\mathbf{r}'|}$$

$$+ \tfrac{1}{2} \int d^3r\, \rho(\mathbf{r}) \int d^3r_1 \int d^3r_2 \frac{n_{PC}(\mathbf{r},\mathbf{r}_1)\, n_{PC}(\mathbf{r},\mathbf{r}_2)}{|\mathbf{r}_1-\mathbf{r}_2|}. \tag{A3}$$

Thus the PC cell is *not* a model for the strong-interaction limit of the exchange-correlation hole; it arises from a different way of dividing up the charge around an electron.

For the uniform electron gas in the strong-interaction limit, the exchange-correlation energy per electron is

$$\tfrac{1}{2} \int d^3r' \frac{n_{xc}(\mathbf{r},\mathbf{r}')}{|\mathbf{r}-\mathbf{r}'|} = -\frac{9}{10r_s}, \tag{A4}$$

while

$$\tfrac{1}{2} \int d^3r' \frac{n_{PC}(\mathbf{r},\mathbf{r}')}{|\mathbf{r}-\mathbf{r}'|} = -\frac{3}{4r_s}. \tag{A5}$$

These are significantly different, although both approaches give the same energy.

For any one-electron system, the exact $n_{xc}(\mathbf{r},\mathbf{r}')$ and the exact $n_{PC}(\mathbf{r},\mathbf{r}')$ (but not their gradient expansions) are equal to one another and to $-\rho(\mathbf{r}')$, so in this limit the two forms of Eq. (A3) are manifestly identical.

APPENDIX B: ELECTROSTATIC POTENTIAL AND ENERGY OF A CHARGED SPHERE WITH A CONSTANT DENSITY GRADIENT

The sphere of radius R has the charge density

$$\rho_{cell}(\mathbf{u}) = (\rho_c + \mathbf{\Gamma} \cdot \mathbf{u})\, \Theta(R-u), \tag{B1}$$

where $u = |\mathbf{u}|$ and $\Theta(t)$ is the step function. ρ_c is the density at the center $\mathbf{u}=0$ of the sphere.

To calculate the electrostatic potential $\Phi_{cell}(\mathbf{u}) = \int d^3r\, \rho_{cell}(\mathbf{r}) |\mathbf{u}-\mathbf{r}|^{-1}$ of this charge distribution at some position $\mathbf{u}$ inside the sphere, we choose the z axis in the direction of $\mathbf{u}$. Then, the x and y terms of $\mathbf{\Gamma} \cdot \mathbf{r} = \Gamma_1 x + \Gamma_2 y + \Gamma_3 z$ in $\rho_{cell}(\mathbf{r})$ do not contribute to the integral $\Phi_{cell}(\mathbf{u})$. Consequently, in spherical coordinates $\{r,\phi,\theta\}$ for $\mathbf{r}$ (with $z = r\cos\theta$),

$$\Phi_{cell}(\mathbf{u}) = 2\pi \int_0^R dr\, r^2 \int_0^\pi d\theta \sin\theta\, [\rho_c + \Gamma_3 r \cos\theta]$$

$$\times \sum_{l=0}^\infty \frac{r_<^l}{r_>^{l+1}} P_l(\cos\theta). \tag{B2}$$

We here have used the multipole expansion of $|\mathbf{u}-\mathbf{r}|^{-1}$ in the usual notation of Ref. [44], where $r_< = \min\{r,u\}$ and $r_> = \max\{r,u\}$. Substituting $t = \cos\theta$, the term in square brackets can be written as $[\rho_c P_0(t) + \Gamma_3 r P_1(t)]$, since the Legendre

polynomials are $P_0(t) \equiv 1$, $P_1(t) \equiv t$, etc. Due to the orthogonality relation $\int_{-1}^{1} dt \, P_m(t) P_n(t) = 2\delta_{m,n}/(2m+1)$, only the $l=0$ and $l=1$ terms contribute to the θ integral of Eq. (B2),

$$\Phi_{cell}(\mathbf{u}) = 4\pi\rho_c \int_0^R dr \frac{r^2}{r_>} + \frac{4\pi}{3} \Gamma_3 \int_0^R dr \frac{r^3 r_<}{r_>^2}. \quad (B3)$$

Γ_3 is the component of $\boldsymbol{\Gamma}$ in the direction of $\mathbf{u}$. We choose the u_3 axis in the direction of $\boldsymbol{\Gamma}$ so that $\Gamma_3 = \Gamma u_3 / u$. The r integrations in (B3) yield

$$\Phi_{cell}(\mathbf{u}) = \frac{2\pi}{3}\rho_c(3R^2 - u^2) + \frac{2\pi}{15}\Gamma u_3(5R^2 - 3u^2)$$

$$(u \leq R). \quad (B4)$$

In the same way, the potential outside the cell is obtained,

$$\Phi_{cell}(\mathbf{u}) = \frac{4\pi}{3}R^3\left(\frac{\rho_c}{u} + \frac{\Gamma R^2}{5}\frac{u_3}{u^3}\right) \quad (u \geq R). \quad (B5)$$

$\Phi_{cell}(\mathbf{u})$ is that solution of the Poisson equation $\nabla^2 \Phi_{cell} = -4\pi\rho_{cell}$ that approaches zero as $u \to \infty$.

The electrostatic self-energy $U_{cell} = \frac{1}{2}\int d^3u \, \Phi_{cell}(\mathbf{u}) \rho_{cell}(\mathbf{u})$ of the sphere with charge density (B1) is easily evaluated in spherical coordinates where $u_3 = u\cos\theta$,

$$U_{cell} = \frac{3}{5}\left(\frac{4\pi}{3}R^3\rho_c\right)^2 R^{-1} + \frac{1}{35}\left(\frac{4\pi}{3}R^3\rho_c\right)^2\left(\frac{\Gamma R}{\rho_c}\right)^2 R^{-1}. \quad (B6)$$

APPENDIX C:
THE PC MODEL FOR THE COEFFICIENT $W_\infty'[\rho]$

We consider oscillations of electrons around a static SCE set of positions $\{\mathbf{r}_i\}_{i=1,\dots,N}$ in a given density $\rho(\mathbf{r})$, as explained in the opening paragraph of Sec. III. If we ignore the collective character of the oscillations as in the Einstein model for phonons, each electron is oscillating independently around an equilibrium position. Since the amplitude of these oscillations asymptotically approaches zero as $\alpha \to \infty$, the PC model still applies. Now, in evaluating the electrostatic energy of the PC cell in Eq. (15) we must merely replace the strictly localized point electron by the smooth charge distribution of an oscillating one. The restoring force on this oscillating electron is the repulsion (scaled by the factor α) by the other $N-1$ electrons, distributed continuously outside a static PC cell, plus the force due to the unknown external potential $v_{ext}^\alpha(\mathbf{r})$. Although the positive background, introduced with Eq. (14), can be used to evaluate the electrostatic energy (15), it is entirely fictitious and, of course, has no effect on the restoring force on the oscillating electron. To obtain this restoring force, we need a model for the true external potential $v_{ext}^\alpha(\mathbf{r})$.

At large $\alpha \gg 1$, $v_{ext}^\alpha(\mathbf{r})$ must become strongly attractive to maintain a given density distribution $\rho(\mathbf{r})$ of the strongly repulsive electrons. In the limit $\alpha \to \infty$ when the kinetic energy becomes negligible, we expect that the strictly correlated electrons are moving on a constant potential-energy surface. For spherical two-electron systems, this can be achieved [8] by

$$v_{ext}^\alpha(\mathbf{r}) \to \alpha \, w(\mathbf{r}) \quad (\alpha \to \infty), \quad (C1)$$

where $w(\mathbf{r})$ is a smooth finite function which is entirely determined by the density $\rho(\mathbf{r})$.

In the PC model for the strictly correlated limit $\alpha \to \infty$, the repulsive force, exerted on the point electron at position $\mathbf{r}$ by the other $N-1$ other electrons, is due to a distribution of continuous *negative* charge with density $\rho(\mathbf{r}')$ outside the PC cell. This force can obviously be canceled exactly by an external force $\mathbf{F}_{ext}^{PC}(\mathbf{r})$ which is chosen as though it was due to an equivalent distribution of continuous *positive* charge with the same density outside the cell. The force $\mathbf{F}_{ext}^{PC}(\mathbf{r})$ is a model for the gradient $-\nabla w(\mathbf{r})$. If it is a conservative force, we can write $\mathbf{F}_{ext}^{PC}(\mathbf{r}) = -\nabla w_{PC}(\mathbf{r})$ where $w_{PC}(\mathbf{r})$ is the PC model for $w(\mathbf{r})$. At least for densities that vary only in the radial or z directions, the construction of $w_{PC}(\mathbf{r})$ is always possible.

To simplify our language, we denote in the following paragraphs by ''$C(\mathbf{x})$'' the spherical region inside the PC cell of a point electron at $\mathbf{r} = \mathbf{x}$ in the strictly correlated limit $\alpha \to \infty$.

In the PC model for strictly correlated motion in the limit $\alpha \to \infty$, the electron carries its PC cell along as it is moving from $\mathbf{r}$ to a close-by position $\mathbf{r} + \mathbf{s}$. Correspondingly, the external force $\mathbf{F}_{ext}^{PC}(\mathbf{r} + \mathbf{s})$ at the new position $\mathbf{r} + \mathbf{s}$ must be calculated from a different distribution of positive charge which is now outside the *new* PC cell $C(\mathbf{r} + \mathbf{s})$. As in the work of Harbola and Sahni [45], we have a position-dependent ''hole'' from which we calculate the electrostatic force at each electron position.

At finite α, in contrast, when the strictly correlated motion is taken to be infinitely slow, there is a *static* PC cell $C(\mathbf{r})$ around an *oscillating* electron. Therefore, as this oscillating electron has moved from its equilibrium position $\mathbf{r}$ to the close-by position $\mathbf{r} + \mathbf{s}$, the external force $\mathbf{F}_{ext}^{PC}(\mathbf{r} + \mathbf{s})$ at $\mathbf{r} + \mathbf{s}$, due to positive charge outside $C(\mathbf{r} + \mathbf{s})$, does *not* cancel the repulsive force due to the other $N-1$ electrons which are still outside the *static* PC cell $C(\mathbf{r})$; see Fig. 3. Consequently, there is a restoring net force $\mathbf{F}_{osc}^{(\mathbf{r})}(\mathbf{s})$. This force can be derived electrostatically from a net charge density $\rho^{(\mathbf{r})}(\mathbf{s})$ which is zero everywhere outside the finite region $C(\mathbf{r}) \cup C(\mathbf{r} + \mathbf{s})$, covered by these two cells. It is the same as a positive charge distribution with density $\rho(\mathbf{r}')$ *inside* $C(\mathbf{r})$, plus a negative charge distribution with density $\rho(\mathbf{r}')$ *inside* $C(\mathbf{r} + \mathbf{s})$.

In the constant-gradient model (17), $\rho^{(\mathbf{r})}(\mathbf{s})$ is the charge distribution of two oppositely charged overlapping spheres $C(\mathbf{r})$ and $C(\mathbf{r} + \mathbf{s})$ with a constant charge-density gradient $\boldsymbol{\Gamma}$ (Fig. 3). The net force exerted by this charge distribution on the oscillating electron at $\mathbf{r} + \mathbf{s}$ is

$$\mathbf{F}_{osc}^{(\mathbf{r})}(\mathbf{s}) = [\nabla_{\mathbf{u}}\Phi_{cell}^{(\mathbf{r})}(\mathbf{u})]_{\mathbf{u} = \mathbf{s} - \mathbf{d}(\mathbf{r})} - [\nabla_{\mathbf{u}}\Phi_{cell}^{(\mathbf{r}+\mathbf{s})}(\mathbf{u})]_{\mathbf{u} = -\mathbf{d}(\mathbf{r}+\mathbf{s})}. \quad (C2)$$
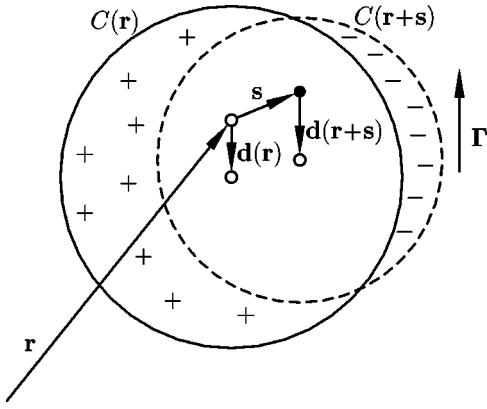
FIG. 3. An electron at $\mathbf{r}+\mathbf{s}$, oscillating around its equilibrium position $\mathbf{r}$, feels a restoring force which is due to a continuous negative charge distribution with density $\rho(\mathbf{r}')$ outside its static PC cell $C(\mathbf{r})$ plus a continuous positive charge distribution with the same density $\rho(\mathbf{r}')$ outside the PC cell $C(\mathbf{r}+\mathbf{s})$. These two different cells are centered at $\mathbf{r}+\mathbf{d}(\mathbf{r})$ and at $(\mathbf{r}+\mathbf{s})+\mathbf{d}(\mathbf{r}+\mathbf{s})$, respectively.

Here, $\Phi_{cell}^{(\mathbf{x})}(\mathbf{u})$ denotes the electrostatic potential at $\mathbf{u}$ due to a spherical piece of positive charge with density (17) inside the PC cell $C(\mathbf{x})$ of an electron with equilibrium position $\mathbf{x}$. The coordinate $\mathbf{u}$ is chosen so that the origin $\mathbf{u}=0$ is at the center of the sphere $C(\mathbf{x})$ and u_3 is the component of the vector $\mathbf{u}$ in the direction of the constant gradient $\mathbf{\Gamma}$. In this coordinate system, the point $\mathbf{x}$ is at $\mathbf{u}=d(\mathbf{x})\,\mathbf{\Gamma}/\Gamma \equiv -\mathbf{d}(\mathbf{x})$ $=\{0,0,d(\mathbf{x})\}$, with $d(\mathbf{r})$ from Eq. (19) (cf. Fig. 2). $\Phi_{cell}^{(\mathbf{x})}(\mathbf{u})$ is explicitly given by Eq. (B4) in Appendix B if we there identify $R=R(\mathbf{x})$, with $R(\mathbf{r})$ from Eq. (19), $\rho_c = \rho(\mathbf{x}) -\Gamma d(\mathbf{x})$, and $\Gamma=|\nabla\rho(\mathbf{x})|$.

As expected, the force (C2) is zero at the equilibrium position $\mathbf{s}=0$. In a uniform system ($\Gamma=0$), where $\mathbf{d}\equiv 0$ and $\Phi_{cell}^{(\mathbf{x})}(\mathbf{u})$ is spherically symmetric around $\mathbf{u}=0$, the second term in (C2) is zero and $\mathbf{F}_{osc}^{(\mathbf{r})}(\mathbf{s})=\nabla_{\mathbf{s}}\Phi_{cell}(\mathbf{s})$. This means that the present approach yields for uniform systems the same zero-point energy as the treatment of zero-point oscillations in a Wigner crystal with a positive background by Ref. [12].

Using expression (B4) from Appendix B, Eq. (C2) can be evaluated explicitly. Expanding the result to linear order in $\mathbf{s}$ yields $\mathbf{F}_{osc}^{(\mathbf{r})}(\mathbf{s})=-\nabla_{\mathbf{s}}v_{osc}^{(\mathbf{r})}(\mathbf{s})$, where the oscillator-type effective potential,

$$v_{osc}^{(\mathbf{r})}(\mathbf{s})=\frac{k_1(\mathbf{r})}{2}(s_1^2+s_2^2)+\frac{k_3(\mathbf{r})}{2}s_3^2, \quad (C3)$$

has $\mathbf{r}$-dependent spring constants

$$k_1(\mathbf{r})=\alpha r_s(\mathbf{r})^{-3}(1-\tfrac{2}{25}\,\gamma^2)+O(\gamma^4), \quad (C4)$$

$$k_3(\mathbf{r})=\alpha r_s(\mathbf{r})^{-3}(1-\tfrac{1}{25}\,\gamma^2)+O(\gamma^4).$$

Here s_3 is the Cartesian component of $\mathbf{s}$ in the direction of $\nabla\rho(\mathbf{r})$, $r_s(\mathbf{r})^{-3}=(4\pi/3)\rho(\mathbf{r})$, and $\gamma=|\nabla\rho(\mathbf{r})|\,r_s(\mathbf{r})/\rho(\mathbf{r})$.

The probability distribution or charge density of an electron performing zero-point oscillations in the potential (C3) is

$$\rho_{osc}^{(\mathbf{r})}(\mathbf{s})=\frac{k_1^{1/2}k_3^{1/4}}{\pi^{3/2}}\exp\{-[k_1^{1/2}(s_1^2+s_2^2)+k_3^{1/2}s_3^2]\}. \quad (C5)$$

Using this charge distribution in evaluating the electrostatic energy (15), we now have instead of Eq. (20)

$$E_{cell,\alpha}^{GEA}([\rho];\mathbf{r})=U_{cell}-\int d^3s\,\Phi_{cell}^{(\mathbf{r})}(\mathbf{s}-\mathbf{d}(\mathbf{r}))\,\rho_{osc}^{(\mathbf{r})}(\mathbf{s}). \quad (C6)$$

To evaluate the $\mathbf{s}$ integral here, we put the s_3 axis in the direction of $\mathbf{\Gamma}$ so that $\mathbf{d}=\{0,0,-d\}$. Setting $\mathbf{u}=\mathbf{s}-\mathbf{d}(\mathbf{r})$ $=\{s_1,s_2,s_3+d\}$ in Eq. (B4) yields

$$\Phi_{cell}^{(\mathbf{r})}(\mathbf{s}-\mathbf{d}(\mathbf{r}))=(\tfrac{3}{2}+\tfrac{4}{50}\,\gamma^2)R^{-1}+\Phi_{odd}(\mathbf{s})$$

$$-\left[(\tfrac{1}{2}+\tfrac{3}{50}\,\gamma^2)\frac{s_1^2+s_2^2}{R^2}\right.$$

$$\left.+(\tfrac{1}{2}+\tfrac{9}{50}\,\gamma^2)\frac{s_3^2}{R^2}\right]R^{-1}+O(\gamma^4). \quad (C7)$$

Here, $\Phi_{odd}(\mathbf{s})$ summarizes the terms containing odd powers of s_1, s_2, or s_3 which do not contribute to the integral in Eq. (C6), since $\rho_{osc}^{(\mathbf{r})}(\mathbf{s})$ is an even function of the s_i. Since $\int d^3s\,\rho_{osc}^{(\mathbf{r})}(\mathbf{s})=1$, the first (constant) term of Eq. (C7) reproduces in Eq. (C6) exactly the expression (21) for $E_{cell}^{GEA}([\rho];\mathbf{r})$. For the contribution $\delta E_{cell,\alpha}^{GEA}([\rho];\mathbf{r})$ of the quadratic term to the integral in Eq. (C6) we note that

$$\int d^3s\,s_i^2\,\rho_{osc}^{(\mathbf{r})}(\mathbf{s})=\frac{k_i^{1/4}}{\pi^{1/2}}\int_{-\infty}^{\infty}ds_i\,s_i^2\,e^{-(k_i^{1/4}s_i)^2}=\frac{1}{2k_i^{1/2}}. \quad (C8)$$

Therefore,

$$\delta E_{cell,\alpha}^{GEA}([\rho];\mathbf{r})=(\tfrac{1}{2}+\tfrac{3}{50}\,\gamma^2)\frac{2}{2R^3k_1^{1/2}}+(\tfrac{1}{2}+\tfrac{9}{50}\,\gamma^2)$$

$$\times\frac{1}{2R^3k_3^{1/2}}+O(\gamma^4). \quad (C9)$$

Since k_1 and k_3 from Eq. (C4) are proportional to α, this contribution is of the order $\alpha^{-1/2}$, as expected. Using the expansions (19), we obtain from Eq. (C4)

$$\frac{1}{R^3k_1^{1/2}}=(1-\tfrac{4}{25}\,\gamma^2)\,r_s(\mathbf{r})^{-3/2}\,\alpha^{-1/2}+O(\gamma^4), \quad (C10)$$

$$\frac{1}{R^3k_3^{1/2}}=(1-\tfrac{9}{50}\,\gamma^2)\,r_s(\mathbf{r})^{-3/2}\,\alpha^{-1/2}+O(\gamma^4).$$

Then, expansion of Eq. (C9) yields

$$E_{cell,\alpha}^{GEA}([\rho];\mathbf{r}) = E_{cell}^{GEA}([\rho];\mathbf{r}) + (\tfrac{3}{4} + \tfrac{1}{40}\gamma^2)$$
$$\times r_s(\mathbf{r})^{-3/2}\alpha^{-1/2} + O(\gamma^4). \quad (C11)$$

Averaging this energy over the density $\rho(\mathbf{r})$ correspondingly to Eq. (15), we obtain the full asymptotics (9) of $W_\alpha[\rho]$ in the PC model, $W_\alpha[\rho] \approx W_\infty^{PC}[\rho] + W'^{PC}_\infty[\rho]\,\alpha^{-1/2}$ ($\alpha \gg 1$), where the coefficients are given by the GEA equations (23) and (24).

While we have not proved that the density $\rho(\mathbf{r})$ is unaffected by the oscillations, we suspect that it is. Clearly

$$\int d^3r\, \rho(\mathbf{r})\, \rho_{osc}^{(\mathbf{r})}(\mathbf{r}' - \mathbf{r}) = \rho(\mathbf{r}') \quad (C12)$$

when $\rho(\mathbf{r}) = \rho(\mathbf{r}') + \nabla\rho(\mathbf{r}')\cdot(\mathbf{r} - \mathbf{r}')$.

APPENDIX D: EXPRESSIONS FOR $W_\infty[\rho]$ AND $W'_\infty[\rho]$ IN LSD, GGA, AND META-GGA

For a given approximate exchange-correlation energy functional $E_{xc}^{app}[\rho] = E_x^{app}[\rho] + E_c^{app}[\rho]$, the corresponding coupling-constant integrand $W_\alpha^{app}[\rho]$ can be found by the following formula [4]:

$$W_\alpha^{app}[\rho_\uparrow,\rho_\downarrow] = E_x^{app}[\rho_\uparrow,\rho_\downarrow] + \frac{d}{d\alpha}(\alpha^2 E_c^{app}[\rho_{\uparrow,1/\alpha},\rho_{\downarrow,1/\alpha}]),$$
$$(D1)$$

where $\rho_{\sigma,1/\alpha}(\mathbf{r}) = \alpha^{-3}\rho_\sigma(\mathbf{r}/\alpha)$ is the spin density scaled uniformly with a parameter $\lambda = 1/\alpha$.

In LSD the correlation energy is written as

$$E_c^{LSD}[\rho_\uparrow,\rho_\downarrow] = \int d^3r\, \rho(\mathbf{r})\varepsilon_c^{unif}(r_s(\mathbf{r}),\zeta(\mathbf{r})), \quad (D2)$$

where $\varepsilon_c^{unif}(r_s,\zeta)$ is the correlation energy per electron of the uniform electron gas with parameters $r_s = (3/4\pi\rho)^{1/3}$, ($\rho = \rho_\uparrow + \rho_\downarrow$), and $\zeta = (\rho_\uparrow - \rho_\downarrow)/(\rho_\uparrow + \rho_\downarrow)$. We are interested in the strictly correlated ($\alpha \to \infty$) limit of LSD. Since $\rho_{1/\alpha}$ is a low density in this limit, we can use the low-density ($r_s \to \infty$) expansion of ε_c^{unif}:

$$\varepsilon_c^{unif}(r_s,\zeta) \xrightarrow{r_s \to \infty} -\frac{d_0(\zeta)}{r_s} + \frac{d_1(\zeta)}{r_s^{3/2}} + O(r_s^{-2}). \quad (D3)$$

Using this expression for the (local) scaled density parameter $r_s^{1/\alpha}(\mathbf{r}) = \alpha r_s(\mathbf{r}/\alpha)$ and inserting into Eq. (D1), one obtains the functionals for the strong-interaction limit [see Eq. (9)] in LSD

$$W_\infty^{LSD}[\rho_\uparrow,\rho_\downarrow] = E_x^{LSD}[\rho_\uparrow,\rho_\downarrow] - \int d^3r\, \rho(\mathbf{r})d_0(\zeta(\mathbf{r}))/r_s(\mathbf{r})$$
$$= -\left(\frac{4\pi}{3}\right)^{1/3}\int d^3r\, d_{xc}(\zeta(\mathbf{r}))\rho(\mathbf{r})^{4/3} \quad (D4)$$

and

$$W'^{\,LSD}_\infty[\rho_\uparrow,\rho_\downarrow] = \frac{1}{2}\left(\frac{4\pi}{3}\right)^{1/2}\int d^3r\, d_1(\zeta(\mathbf{r}))\rho(\mathbf{r})^{3/2}. \quad (D5)$$

For the coefficients d_0 and d_{xc} in Eq. (D4) we use the low-density limit of the parametrization of $\varepsilon_c^{unif}(r_s,\zeta)$ suggested by Perdew and Wang [37]. $d_{xc}(\zeta)$ is then given by Eq. (28) of Ref. [37] and d_0 by

$$d_0(\zeta) = d_{xc}(\zeta) - \frac{3}{8\pi}\left(\frac{9\pi}{4}\right)^{1/3}[(1+\zeta)^{4/3} + (1-\zeta)^{4/3}]. \quad (D6)$$

One finds that $d_{xc}(\zeta)$ is very close to 0.9, the value for the PC model, and almost independent of the spin polarization (see Table IV of Ref. [37]). On the other hand, the coefficient d_1 obtained from the Perdew-Wang parametrization varies as a function of ζ from $d_1(\zeta=0) = 1.4408$ to $d_1(\zeta=1) = 1.7697$. However, just as for d_{xc}, we expect the exact coefficient d_1 to be independent of ζ, because in a low-density electron gas any two electrons will avoid one another, no matter how their spins are aligned relative to one another. In Eq. (D5) and the corresponding expressions for GGA and MGGA [Eqs. (D14) and (D16)], we will therefore use the spin-independent coefficient from the PC model, $d_1 = 1.5$, which we believe to be more correct. Thus, in Tables I–VI, all our functionals for W_∞ and W'_∞ will agree closely for a uniform density.

In the GGA of Perdew, Burke, and Ernzerhof, the correlation energy functional is given by Eqs. (3), (7), and (8) of Ref. [26]. Under uniform scaling to the low-density limit, the function A given by Eq. (8) of Ref. [26] scales to

$$A(\alpha r_s,\zeta) \xrightarrow{\alpha \to \infty} B_1(r_s,\zeta)\alpha + B_2(r_s,\zeta)\alpha^{1/2} + O(\alpha^0), \quad (D7)$$

with

$$B_1(r_s,\zeta) = \frac{\beta}{d_0(\zeta)}\phi(\zeta)^3 r_s \quad (D8)$$

and

$$B_2(r_s,\zeta) = \frac{\beta\, d_1(\zeta)}{d_0(\zeta)^2}\phi(\zeta)^3\, r_s^{1/2}. \quad (D9)$$

Here, $\beta = 0.066\,725$ is the coefficient of the second-order gradient expansion of the correlation energy of a slowly varying electron gas, $\phi(\zeta) = [(1+\zeta)^{2/3} + (1-\zeta)^{2/3}]/2$, and d_0 and d_1 are the coefficients of the low-density expansion of $\varepsilon_c^{unif}(r_s,\zeta)$.

In the same low-density limit, the function H given by Eq. (7) of Ref. [26] scales as

$$H(\alpha r_s,\zeta,\alpha^{1/2}t) \xrightarrow{\alpha \to \infty} H_1(r_s,\zeta,t)\alpha^{-1} + H_2(r_s,\zeta,t)\alpha^{-3/2}$$
$$+ O(\alpha^{-2}), \quad (D10)$$

where $t=|\nabla\rho|/[2\phi(\zeta)k_s\rho]$ is a reduced density gradient with $k_s=\sqrt{4k_F/\pi}$ and $k_F=(3\pi^2\rho)^{1/3}$. The functions H_1 and H_2 are defined by

$$H_1(r_s,\zeta,t)=\beta\phi(\zeta)^3t^2\frac{1+B_1t^2}{1+B_1t^2+B_1^2t^4} \qquad (D11)$$

and

$$H_2(r_s,\zeta,t)=-\beta\phi(\zeta)^3B_1B_2t^6\frac{2+B_1t^2}{(1+B_1t^2+B_1^2t^4)^2}. \qquad (D12)$$

Insertion into Eq. (D1) then yields

$$W_\infty^{GGA}[\rho_\uparrow,\rho_\downarrow]=E_x^{GGA}[\rho_\uparrow,\rho_\downarrow]+\int d^3r\,\rho(\mathbf{r})\left(-\frac{d_0(\zeta(\mathbf{r}))}{r_s(\mathbf{r})}\right.$$
$$\left.+H_1(r_s(\mathbf{r}),\zeta(\mathbf{r}),t(\mathbf{r}))\right), \qquad (D13)$$

$$W_\infty'^{\,GGA}[\rho_\uparrow,\rho_\downarrow]=\frac{1}{2}\int d^3r\,\rho(\mathbf{r})\left(\frac{d_1(\zeta(\mathbf{r}))}{r_s(\mathbf{r})^{3/2}}\right.$$
$$\left.+H_2(r_s(\mathbf{r}),\zeta(\mathbf{r}),t(\mathbf{r}))\right). \qquad (D14)$$

Equations (D10)–(D12) can also be used to calculate the low-density limit of the correlation energy in meta-GGA [Eq. (15) of Ref. [27]]. The results are

$$W_\infty^{MGGA}[\rho_\uparrow,\rho_\downarrow]=E_x^{MGGA}[\rho_\uparrow,\rho_\downarrow]+\int d^3r\left\{\rho(\mathbf{r})\left(-\frac{d_0(\zeta(\mathbf{r}))}{r_s(\mathbf{r})}+H_1(r_s(\mathbf{r}),\zeta(\mathbf{r}),t(\mathbf{r}))\right)\left[1+C\left(\frac{\sum_\sigma\tau_\sigma^W}{\sum_\sigma\tau_\sigma}\right)^2\right]\right.$$

$$\left.-(1+C)\sum_\sigma\rho_\sigma(\mathbf{r})\left(\frac{\tau_\sigma^W}{\tau_\sigma}\right)^2\left(-\frac{d_0(1)}{r_{s,\sigma}(\mathbf{r})}+H_1(r_{s,\sigma}(\mathbf{r}),1,t_\sigma(\mathbf{r}))\right)\right\} \qquad (D15)$$

and

$$W_\infty'^{\,MGGA}[\rho_\uparrow,\rho_\downarrow]=\frac{1}{2}\int d^3r\left\{\rho(\mathbf{r})\left(\frac{d_1(\zeta(\mathbf{r}))}{r_s(\mathbf{r})}+H_2(r_s(\mathbf{r}),\zeta(\mathbf{r}),t(\mathbf{r}))\right)\left[1+C\left(\frac{\sum_\sigma\tau_\sigma^W}{\sum_\sigma\tau_\sigma}\right)^2\right]\right.$$

$$\left.-(1+C)\sum_\sigma\rho_\sigma(\mathbf{r})\left(\frac{\tau_\sigma^W}{\tau_\sigma}\right)^2\left(\frac{d_1(1)}{r_{s,\sigma}(\mathbf{r})}+H_2(r_{s,\sigma}(\mathbf{r}),1,t_\sigma(\mathbf{r}))\right)\right\}. \qquad (D16)$$

Here

$$\tau_\sigma^W=\frac{1}{8}\frac{|\nabla\rho_\sigma|^2}{\rho_\sigma} \qquad (D17)$$

is the Weizsäcker kinetic energy density,

$$\tau_\sigma=\frac{1}{2}\sum_i^{occup}|\nabla\varphi_{i\sigma}|^2 \qquad (D18)$$

is the kinetic energy density of the Kohn-Sham orbitals $\varphi_{i\sigma}$, $C=0.53$ is a constant parameter, and $r_{s,\sigma}$ and t_σ are constructed like r_s and t, but using ρ_σ instead of ρ.

APPENDIX E: SOFT-PLASMON INSTABILITY OF THE LOW-DENSITY UNIFORM ELECTRON GAS

The low-density uniform electron gas (neutralized by a rigid uniform background) is unstable against the formation of a body-centered-cubic (bcc) Wigner crystal, or equivalently against the formation of a charge-density wave of wave vector $Q\approx1.14(2k_F)$ (the smallest nonzero reciprocal-lattice vector of the bcc crystal), where $\bar\rho=k_F^3/3\pi^2$ is the uniform density. Perdew and Datta [46] have shown that, starting from the uniform phase, the density variation

$$\delta\rho(z)=\bar\rho A\cos(Qz) \qquad (E1)$$

of small amplitude A produces an energy change per electron

$$\frac{\delta E}{N} = e(k_F, Q)A^2 + O(A^4), \qquad \text{(E2)}$$

where the coefficient e is given by their Eq. (43). $e < 0$ indicates instability against the formation of a charge-density wave of infinitesimal amplitude.

In the limit $\bar{\rho} \to 0$, in which the wave function $\Psi_\alpha[\rho]$ for all $\alpha > 0$ is correlated as in the strong-interaction limit ($\alpha \to \infty$), Eq. (2) implies that $E_{xc} = W_\infty$. Using our PC expression (23) for W_∞, Eq. (43) of Ref. [46] becomes

$$e = \frac{k_F}{12\pi x^2}[1 - 1.965x^2 + 1.241x^4], \qquad \text{(E3)}$$

where $x = Q/2k_F$. The first term of Eq. (E3) arises from the Hartree electrostatic energy, the second from the local part of E_{xc}, and the third from the second-order gradient contribu-

tion to $E_{xc} = W_\infty$. Equation (E3) is always positive but has a minimum very close to zero at $x \approx 1$ or $Q \approx 2k_F$. Thus our PC gradient expansion almost predicts the correct low-density instability of the uniform electron gas.

This instability can also be regarded as a ``soft plasmon'': The plasmon frequency $\omega_p(Q)$ decreases from $\omega_p(0) = \sqrt{4\pi\bar{\rho}}$ as Q increases, and goes to zero around $Q = 2k_F$. Within the PC model, the low-density limit for the plasmon dispersion is $\omega_P(Q) = \omega_P(0)(1 - 1.965x^2 + 1.241x^4)^{1/2}$, consistent with Fig. 2 of Ref. [47]. Figure 5 of Ref. [48] suggests that the plasmon dispersion changes sign around $r_s = 10$, although the soft-plasmon instability appears around $r_s = 65$ [49].

If the electron-electron interaction were attractive, the Hartree term in Eq. (E3) would be negative. Then Eq. (43) of Ref. [46] shows that the uniform phase for *any* $\bar{\rho}$ would be unstable against long-wavelength ($Q \to 0$ or $x \to 0$) charge-density waves.

---

[1] R. G. Parr and W. Yang, *Density-Functional Theory of Atoms and Molecules* (Oxford University Press, New York, 1989).

[2] D. C. Langreth and J. P. Perdew, Solid State Commun. **17**, 1425 (1975).

[3] O. Gunnarsson and B. I. Lundqvist, Phys. Rev. B **13**, 4274 (1976).

[4] A. Görling and M. Levy, Phys. Rev. B **47**, 13 105 (1993); Phys. Rev. A **52**, 4493 (1995).

[5] M. Levy and J. P. Perdew, Phys. Rev. A **32**, 2010 (1985).

[6] M. Seidl, J. P. Perdew, and M. Levy, Phys. Rev. A **59**, 51 (1999).

[7] M. Seidl, J. P. Perdew, and S. Kurth, Phys. Rev. Lett. (to be published).

[8] M. Seidl, Phys. Rev. A **60**, 4387 (1999).

[9] P. Ziesche, J. Tao, M. Seidl, and J. P. Perdew, Int. J. Quantum Chem. **77**, 819 (2000).

[10] M. Seidl and J. P. Perdew, Phys. Rev. B **50**, 5744 (1994).

[11] E. Wigner, Trans. Faraday Soc. **34**, 678 (1938).

[12] D. Pines, *Elementary Excitations in Solids* (W. A. Benjamin, New York, 1964).

[13] S. M. Valone, Phys. Rev. B **44**, 1509 (1991).

[14] M. Levy and J. P. Perdew, Phys. Rev. B **48**, 11 638 (1993); **55**, 13 321(E) (1997).

[15] M. Ernzerhof, J. P. Perdew, and K. Burke, Int. J. Quantum Chem. **64**, 285 (1997).

[16] J. P. Perdew, M. Ernzerhof, and K. Burke, J. Chem. Phys. **105**, 9982 (1996).

[17] M. Ernzerhof, Chem. Phys. Lett. **263**, 499 (1996).

[18] K. Burke, M. Ernzerhof, and J. P. Perdew, Chem. Phys. Lett. **265**, 115 (1997).

[19] R. Q. Hood, M. Y. Chou, A. J. Williamson, G. Rajagopal, and R. G. Needs, Phys. Rev. B **57**, 8972 (1998).

[20] D. P. Joubert and G. P. Srivastava, J. Chem. Phys. **109**, 5212 (1998).

[21] F. Colonna and A. Savin, J. Chem. Phys. **110**, 2828 (1999).

[22] K. Burke (private communication).

[23] A. D. Becke, J. Chem. Phys. **98**, 1372 (1993).

[24] P. Fulde, *Electron Correlations in Molecules and Solids* (Springer, Berlin, 1993), see section 8.4.

[25] H. B. Shore, E. Zaremba, J. H. Rose, and L. Sander, Phys. Rev. B **18**, 6506 (1978).

[26] J. P. Perdew, K. Burke, and M. Ernzerhof, Phys. Rev. Lett. **77**, 3865 (1996); **78**, 1396 (1997).

[27] J. P. Perdew, S. Kurth, A. Zupan, and P. Blaha, Phys. Rev. Lett. **82**, 2544 (1999); **82**, 5179(E) (1999).

[28] J. P. Perdew, K. Burke, and Y. Wang, Phys. Rev. B **54**, 16 533 (1996); **57**, 14 999 (1998); and references therein.

[29] P. R. Antoniewicz and L. Kleinman, Phys. Rev. B **31**, 6779 (1985).

[30] S.-K. Ma and K. A. Brueckner, Phys. Rev. **165**, 18 (1968).

[31] D. J. W. Geldart and M. Rasolt, Phys. Rev. B **13**, 1477 (1976).

[32] D. C. Langreth and J. P. Perdew, Phys. Rev. B **21**, 5469 (1980).

[33] R. A. Coldwell-Horsfall and R. A. Maradudin, J. Math. Phys. **1**, 395 (1960).

[34] W. J. Carr, R. A. Coldwell-Horsfall, and A. E. Fein, Phys. Rev. **124**, 747 (1961).

[35] F. Herman and N. H. March, Solid State Commun. **50**, 725 (1984).

[36] D. Ceperley, Phys. Rev. B **18**, 3126 (1978).

[37] J. P. Perdew and Y. Wang, Phys. Rev. B **45**, 13 244 (1992).

[38] J. P. Perdew, A. Savin, and K. Burke, Phys. Rev. A **51**, 4531 (1995).

[39] A. Svane and O. Gunnarsson, Phys. Rev. Lett. **65**, 1148 (1990).

[40] M. T. Czyżyk and G. A. Sawatzky, Phys. Rev. B **49**, 14 211 (1994).

[41] L. Pollack and J. P. Perdew, J. Phys.: Condens. Matter **12**, 1239 (2000).

[42] J. P. Perdew, S. Kurth, and M. Seidl, in *Advances in Quantum Many-Body Theory*, edited by R. F. Bishop, K. A. Gernoth, N.

R. Walet, and Y. Xian (World Scientific, Singapore, in press), Vol. 3.

[43] J. Rey and A. Savin, Int. J. Quantum Chem. **69**, 581 (1998).

[44] J. D. Jackson, *Classical Electrodynamics*, 2nd ed. (Wiley, New York, 1975).

[45] M. K. Harbola and V. Sahni, Phys. Rev. Lett. **62**, 489 (1989).

[46] J. P. Perdew and T. Datta, Phys. Status Solidi B **102**, 283 (1980).

[47] K. S. Singwi, M. P. Tosi, R. H. Land, and A. Sjölander, Phys. Rev. **176**, 589 (1968).

[48] P. Vashishta and K. S. Singwi, Phys. Rev. B **6**, 875 (1972).

[49] G. Ortiz, M. Harris, and P. Ballone, Phys. Rev. Lett. **82**, 5317 (1999).

[50] J. B. Krieger, Y. Li, and G. J. Iafrate, Phys. Rev. A **45**, 101 (1992).

[51] M. Ernzerhof (private communication) (method of Ref. [17]).

[52] E. Engel and R. M. Dreizler, J. Comput. Chem. **20**, 31 (1999).

[53] R. D. Amos, I. L. Alberts, J. S. Andrews, S. M. Colwell, N. C. Handy, D. Jayatilaka, P. J. Knowles, R. Kobayashi, G. J. Laming, A. M. Lee, P. E. Maslen, C. W. Murray, P. Palmieri, J. E. Rice, J. Sanz, E. D. Simandiras, A. J. Stone, M.-D. Su, and D. J. Tozer, CADPAC6: The Cambridge Analytical Derivatives Package Issue 6.0 Cambridge, 1995.

[54] E. S. Kryachko and E. V. Ludeña, *Energy Density Functional Theory of Many-Electron Systems* (Kluwer, Dordrecht, 1990).